Enhanced Overhead Crane Control using ADRC and ZVD Input Shaping with Trajectory Planning

Van Dong Nguyen
School of Electrical and Electronic Engineering
Hanoi University of Science and Technology
Vietnam

Minh Duc Duong
School of Electrical and Electronic Engineering
Hanoi University of Science and Technology
Vietnam

Trong Hieu Do
School of Electrical and Electronic Engineering
Hanoi University of Science and Technology
Vietnam

Overhead crane control with time-varying cable length presents significant challenges, particularly in maintaining accurate trolley positioning while minimizing residual payload oscillations induced by lifting and lowering operations. This paper proposes a hybrid control approach combining Active Disturbance Rejection Control (ADRC) with Zero Vibration Derivative (ZVD) input shaping to address these issues. ADRC enhances system robustness against external disturbances and model uncertainties, providing stable tracking performance. However, due to its limitations in completely suppressing residual oscillations, the ZVD input shaper is integrated to reduce payload sway. To further optimize shaping performance under variable rope lengths, an average cable length strategy is employed for parameter tuning. Additionally, a reference trajectory planning scheme is developed to smooth command inputs, reducing sudden impacts, induced oscillations, and improving overall system stability during crane operation.

Keywords: *Overhead crane, vibration control, ADRC; input shaping; trajectory planning, disturbance rejection;*

1. INTRODUCTION

Overhead cranes are indispensable transportation devi–ces in various industrial sectors, particularly in manu–facturing and logistics, where high precision and ope–rational efficiency are required [1]. One of the main challenges in crane control arises from the dynamic structure of the system. Specifically, the payload is not directly actuated but is instead influenced by the motion of the trolley through a suspended cable mechanism. This results in an under actuated system with more degrees of freedom than available control inputs, increasing the complexity of trajectory control and residual vibration suppression. Moreover, the payload may vary over time due to operational requirements, introducing uncertainty into the system dynamics. Without an appropriate control strategy, residual vibrations generated during motion can degrade positioning accuracy, prolong transportation time, and compromise equipment safety. Therefore, developing effective control solutions to minimize residual vibrations and enhance operational performance remains a critical issue.

There has been significant research on the regulation of overhead crane systems, resulting in a wide range of control methodologies [2]. Open-loop strategies, such as the widely used input shaping technique [3, 4], can efficiently suppress load oscillations and are relatively simple to implement. Another approach employs flatness theory to handle the under actuated dynamics of crane systems by mapping system inputs and states to flat outputs [5]. However, such open-loop methods ge–nerally demonstrate limited effectiveness in the pre–sence of external disturbances. Moreover, most existing studies have primarily focused on minimizing payload oscillations, whereas in real-world operations, cranes are often required to transport loads precisely to specific target positions. Another direction focuses on closed-loop control, a methodology that offers greater precision in system regulation. Several feedback control strategies have been proposed for crane systems, including PSO-based nonlinear feedback control [6], nonlinear quasi-PID control [7], and model predictive control [8], all of which improve positioning accuracy and system stability. Recently, there has been increasing interest in advanced control techniques based on fuzzy logic models, as highlighted in [9]. However, the design and tuning of such controllers often require specialized expertise from experienced engineers. While many of these methods have demonstrated success in controlling crane systems and reducing load oscillations, achieving high-precision control using feedback controllers typically requires multiple sensors to monitor both the trolley position and the payload swing angles. However, the integration of these additional sensors increases system cost and introduces complexity in accurately measuring payload angles. This challenge arises from variations in payload masses, dimensions, and configurations, which can adversely affect sensor performance and overall system reliability.

In crane operations, it is often necessary to transport loads while simultaneously raising or lowering them to enhance efficiency or avoid obstacles [10, 11]. This dynamic motion leads to fluctuations in the rope length, which in turn causes variations in the vibration frequency of the payload. In this paper, we propose a hybrid control strategy based on Active Disturbance

Received: April 2025, Accepted: May 2025
Correspondence to: Dr Trong Hieu Do
Hanoi University of Science and Technology,
No. 1 Dai Co Viet, Hai Ba Trung, Hanoi, Vietnam
E-mail: hieu.dotrong@hust.edu.vn
doi: 10.5937/fme2503363D

Rejection Control (ADRC) integrated with a modified zero-vibration derivative shaper for a two-dimensional overhead crane system featuring adjustable cable length. The proposed method is designed to enhance robustness against model uncertainties and external disturbances while minimizing the dependency on additional sensors. Unlike conventional model-based approaches, the ADRC framework offers real-time disturbance estimation and compensation, enabling more accurate and reliable control for under actuated overhead cranes with varying cable lengths. Recently, Active Distur–bance Rejection Control (ADRC) has emerged as a powerful and effective strategy for addressing chal–lenges in control systems. Since its introduction by Han [12, 13], ADRC has attracted considerable attention as a potential alternative to the traditional PID controller. As a modern control methodology, ADRC focuses on real-time estimation and rejection of disturbances without requiring an accurate mathematical model of the system. ADRC operates based on three key components: an Extended State Observer (ESO), which estimates both system states and total disturbances; a linear feedback controller, which adjusts the control input to ensure fast and stable responses; and a disturbance compensation mechanism, which mitigates the effects of disturbances on the system output. This approach is particularly well-suited for nonlinear systems subjected to unknown dis–turbances, offering high accuracy and strong adap–tability. ADRC has been simplified into an industrially applicable model, with its implementation made more intuitive through a controller parameter tuning method based on observer bandwidth, as proposed in [14]. Alt–hough ADRC has shown its effectiveness in improving disturbance rejection capability and adaptability to load variations, residual vibrations may still occur due to the dynamic characteristics of the crane system. To over–come this limitation, integrating ADRC with Input Sha–ping and a well-designed reference trajectory to smooth the control input is a promising approach. In this framework, ADRC ensures control performance by estimating and compensating for disturbances in real time, input shaping suppresses residual vibrations at the control input level, and the carefully designed reference trajectory minimizes abrupt impacts on the system. This combination not only enhances positioning accuracy but also maintains operational speed, significantly impro–ving overall control quality of the crane system. In summary, the contributions of this paper are as follows:

- A trolley position controller is developed based on ADRC to regulate the trolley to the desired position while effectively minimizing disturbances caused by payload oscillations.
- A cable length control strategy, combining ADRC with trajectory planning, is proposed to control the payload's vertical motion and safely avoid fixed obstacles during lifting and lowering.
- An improved input shaping method is integrated to suppress payload oscillations during motion and reduce residual vibrations, while maintaining a simple and practical controller design.

The subsequent parts of the paper are structured as outlined below: Section 2 presents the mathematical model of the overhead crane. Section 3 illustrates the design of the proposed control system. The simulation and experiment scenarios were introduced in section 4. Finally, some conclusions end the document.

2. OVERHEAD CRANE DYNAMIC MODEL

To analyze and design the overhead crane control system, it is essential to first establish a dynamic model that accurately describes the movement of the trolley and the payload. The crane system is modeled in a two-dimensional plane, where the trolley moves along the x-axis, and the payload undergoes combined horizontal and vertical motion as a result of the trolley displacement and rope length variation. The sway angle defines the payload's relative position with respect to the trolley. This configuration is illustrated in Figure 1. Due to the non-linearity of the system and control constraints, the model must comprehensively capture the dynamic relationships among the state variables, including the position and velocity of the trolley, the length of the cable, and the oscillation of the payload. Specifically:

- x: position of the trolley
- l: length of the suspension cable
- θ : oscillation angle of the payload
- m_t: mass of the trolley
- m_p : mass of the payload

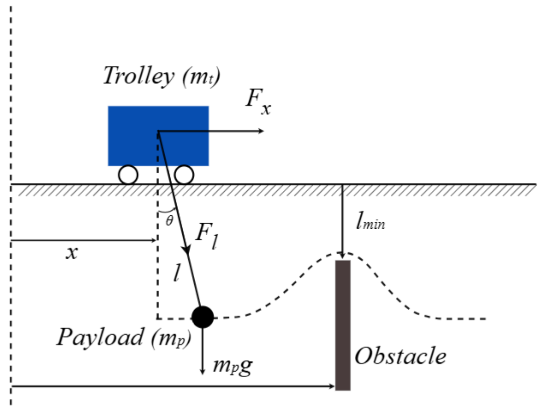

Figure 1. Model of a 2D overhead crane with obstacle-avoidance trajectory

Based on the assumptions that both the trolley and payload are modeled as point masses and the mass and elasticity of the cable are neglected, the system's dyna–mic equations are derived using the Lagrange method. Specifically, by determining the system's kinetic and potential energies and applying the generalized Lag–range equation, a set of nonlinear differential equations is obtained to describe the motion of the trolley and payload under the influence of control forces. The deta–iled dynamic equations are presented as follows [15]:

$$\begin{cases} \left(m_t + m_p\right) + m_p\dot{l}\sin\theta + 2m_p\dot{l}\dot{\theta}\cos\theta \\ -m_p l\theta^2\sin\theta + m_p l\ddot{\theta}\cos\theta = F_x - b_x\dot{x} \\ m_p\dot{l} + m_p\ddot{x}\sin\theta - m_p l\dot{\theta} - m_p g\cos\theta = \\ \qquad = F_l - b_l\dot{l}, \# \\ \quad m_p l^2\ddot{\theta} + m_p l\ddot{x}\cos\theta - 2m_p l\dot{l}\dot{\theta} \\ \qquad + m_p gl\sin\theta = -c_0\dot{\theta} \# \end{cases} \tag{1}$$

where b_x is the damping coefficient of the trolley along the x-axis, b_l is the damping coefficient of the cable along the y-axis, and c_0 is the rotational damping coefficient affecting the payload oscillation.

In practical applications, overhead crane systems may encounter obstacles along the trajectory of the pay–load, as illustrated in Figure 1. To ensure safe and effi–cient load transportation, this paper proposes a control strategy designed to enable obstacle avoidance while meeting the following specific operational require–ments:

- The trolley moves from the initial position x_i to the desired position x_d, with an initial cable length of l_{max}.
- Given an obstacle located at position x_b, the control strategy must ensure that the payload is lifted to at least l_{min} when the trolley reaches x_b, and subse–quently lowered back to the initial height l_{max} when the trolley arrives at x_d.
- The payload oscillation must be suppressed throughout the entire motion, ensuring no residual vibration upon reaching the final position.

In the next section, we will introduce a control app–roach for enhancing the operation of the overhead crane system, ensuring that the payload follows the de–sired trajectory while eliminating residual oscillations.

3. CONTROL STRATEGY

To enhance the control performance, this paper pro–poses the application of the ADRC controller to imp–rove disturbance rejection capability and system accuracy. Simultaneously, the Zero Vibration Deriva–tive (ZVD) shaper is integrated to eliminate payload oscillations during transportation. Additionally, the reference trajectory is designed to smooth the control input, ensuring seamless system operation and mini–mizing sudden impacts on the actuation mechanism, thereby improving system durability and stability. The proposed control structure of the crane system is presented in Figure 2.

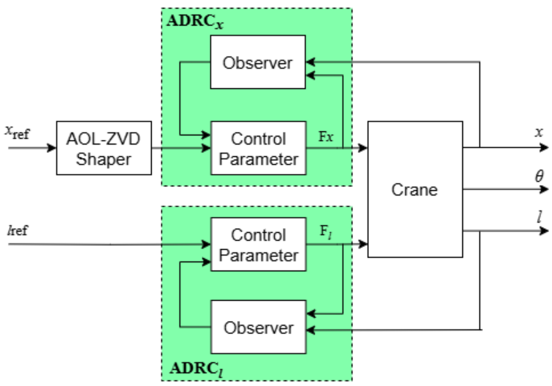

Figure 2. Control structure design

The overhead crane dynamics is divided into actu–ated and unactuated components. The tracking control dynamics are designed based on the actuated component to move the trolley and load accurately along the desired trajectory. For the unactuated component, the ZVD input shaping technique is incorporated to minimize load oscillations during operation. Input shaping is an effective and simple vibration control technique that does not require significant alterations to the existing control structure. For dealing with the variation in payload vibration frequencies caused by cable length changes, the average operating length ZVD (AOL-ZVD) is used, where the natural frequency is calculated based on the average of the minimum length and the maximum length of the cable during the hoisting/lowering process.

3.1 Active disturbance rejection control

The ADRC method is an advanced control strategy in which system models are extended by introducing a new state variable. This state variable encapsulates all unk–nown dynamics and residual disturbances that are not included in the conventional system description. The new state is estimated through the application of an Extended State Observer (ESO), which is responsible for tracking and estimating external disturbances as well as model uncertainties that deviate from real-world con–ditions. The theoretical foundation of the ADRC controller is presented in detail in [13, 16].

The equations in (1) are rewritten in the form as:

$$\ddot{x}(t) = f_x + b_{0x}F_x = f_x + \frac{1}{m_t + m_p}F_x \tag{2}$$

$$\ddot{l}(t) = f_l + b_{0l}F_l = f_l + \frac{1}{m_p}F_l \tag{3}$$

where:

$$f_x = -\left(m_p\ddot{l}\sin\theta + 2m_p\dot{l}\dot{\theta}\cos\theta - \right.$$
$$\left. -m_p l\dot{\theta}^2\sin\theta + m_p l\ddot{\theta} + b_x\dot{x}\right)$$
$$f_l = -\left(m_p\ddot{x}\sin\theta - m_p l\dot{\theta}^2 - m_p g\cos\theta + b_l l\right)/m_p$$

Generally, f_x and f_l comprise nonlinearities and pa–rameter uncertainties, constituting a combined distur–bance. Equations (2) and (3) exhibit the standard confi–guration of a second-order system, characterized by the following form, where $y(t)$ represents the output while $u(t)$ is the control signal and ft) is general disturbances:

$$\ddot{y}_t = f(t) + b_0 u(t) \tag{4}$$

The fundamental concept of ADRC is to implement an Extended State Observer (ESO) to provide an esti–mate $\hat{f}(t)$ enabling compensation for the effect of if $f(t)$ on the system model by disturbance rejection. To obtain this estimate, we rewrite (4) in the state-space representation:

$$\begin{bmatrix}\dot{x}_1(t)\\ \dot{x}_2(t)\\ \dot{x}_3(t)\end{bmatrix} = \underbrace{\begin{bmatrix}0 & 1 & 0\\ 0 & 0 & 1\\ 0 & 0 & 0\end{bmatrix}}_{A}\begin{bmatrix}x_1(t)\\ x_2(t)\\ x_3(t)\end{bmatrix} + \underbrace{\begin{bmatrix}0\\ b_0\\ 0\end{bmatrix}}_{B}u(t) + \underbrace{\begin{bmatrix}0\\ 0\\ 1\end{bmatrix}}_{C}\dot{f}(t) \tag{5}$$
$$y(t) = \begin{bmatrix}1 & 0 & 0\end{bmatrix}\begin{bmatrix}x_1(t)\\ x_2(t)\\ x_3(t)\end{bmatrix}$$

With l_1, l_2 and l_3 as the parameters of the ESO, which are determined such that $\hat{x}_1$, $\hat{x}_2$, and $\hat{x}_3$ estimate y, $\dot{y}$, and f, respectively. The model of the extended state ob–server is constructed as follows:

$$\begin{bmatrix}\hat{x}_1(t)\\ \hat{x}_2(t)\\ \hat{x}_3(t)\end{bmatrix}=\underbrace{\begin{bmatrix}-l_1 & 1 & 0\\ -l_2 & 0 & 1\\ -l_3 & 0 & 0\end{bmatrix}}_{A-LC}\begin{bmatrix}\hat{x}_1(t)\\ \hat{x}_2(t)\\ \hat{x}_3(t)\end{bmatrix}+\underbrace{\begin{bmatrix}0\\ b_0\\ 0\end{bmatrix}}_{B}u(t)+\begin{bmatrix}l_1\\ l_2\\ l_3\end{bmatrix}y(t) \quad (6)$$

The state feedback control law is then based on the estimate:

$$\begin{aligned} u(t) &= \frac{u_0 - \hat{x}_3(t)}{b_0} \\ u_0(t) &= K_p\left(r(t)-\hat{x}_1(t)\right)-K_D\hat{x}_2(t) \end{aligned} \quad (7)$$

By substituting (7) into (4), we obtain:

$$\ddot{y} \approx\sim u_0(t) = K_p\left(r(t)-y(t)\right)-K_D\dot{y}(t) \quad (8)$$

Taking the Laplace transform of 8, the closed-loop transfer function is obtained as follows:

$$G(s)=\frac{Y(s)}{R(s)}=\frac{K_p}{s^2+K_D s+K_p} \quad (9)$$

The second-order ADRC control loop structure is shown in Figure 3.

With T_{settle} being the desired settling time of the system, the parameters are calculated as follows:

$$\begin{cases} s^{CL} \approx \dfrac{\sim -5.85}{T_{settle}}, K_p = \left(S^{CL}\right)^2, K_D = -2s^{CL} \\ l_1 = -3s^{ESO}, l_2 = 3\left(s^{ESO}\right)^2, l_3 = -\left(s^{ESO}\right)^3 \\ s^{ESO} \approx\sim k \cdot s^{CL}, k > 1 \end{cases} \quad (10)$$

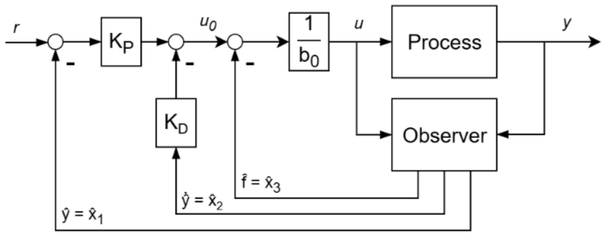

Figure 3. Second-Order ADRC Control Model.

3.2 Modified input shaping

Input Shaping is an effective control method used to manage and reduce vibrations in dynamic systems [17, 18]. This method is notable for its simplicity, ease of design and implementation, and its broad applicability across various types of systems. The input shaping algorithm improves system performance and accuracy by adjusting the input signal to minimize unwanted oscillations. The core idea of input shaping is to apply a series of pulses with appropriate magnitude and timing so that these pulses interact with the system in a way that cancels each other out, thereby completely elimi–nating the vibration. In this paper, the input shaping method is implemented using three pulses (Zero Vibra–tion Derivative - ZVD), which effectively cancel the oscillations and improve the stability of the overhead crane system during operation.

The Input Shaping algorithm is formulated based on the dynamic model of a second-order oscillatory sys–tem, which is represented by the following transfer function:

$$\frac{Y(s)}{U(s)}=\frac{\omega_n^2}{s^2+2\zeta\omega_n+\omega_n^2} \quad (11)$$

in which ω_{in} is the natural frequency of oscillation, and ζ is the damping ratio. If an impulse $u_i(t) = A_i\zeta(t-t_i)$ is applied at time t_i with an amplitude of A_i, the system output is given by:

$$y_i(t)=A_i\frac{\omega_n}{\sqrt{1-\zeta^2}}e^{-\zeta\omega(t-t_i)}\sin\left(\omega_n\sqrt{1-\zeta^2}\left(-t_i\right)\right) \quad (12)$$

One approach to implementing the Input Shaping technique is through impulse vectors [19]. The osci–llatory response governed by equation 11, with an input impulse $u_i(t) = A_i\zeta(t-t_i)$, is represented in vector form as shown in Figure 4. If the impulse amplitude is positive ($A_i > 0$), the impulse vector originates from the coor–dinate origin. Conversely, if the impulse amplitude is negative ($A_i < 0$), the impulse vector terminates at the coordinate origin.
where:

$$\begin{cases} I_i = A_i e^{\zeta\omega_n t_i} \\ \theta_1 = \omega_d t_i \end{cases} \quad (13)$$

with:

- A_i denotes the impulse amplitude.
- t_i represents the impulse timing.
- $\omega_d = \omega_n\sqrt{1-\zeta^2}$ is the damped natural frequency.

Figure 5 illustrates the impulse vector diagram of the ZVD shaper. The ZVD shaper consists of three im–pulses, where the first impulse vector is located at 0, the second impulse vector at π, and the third impulse vector at 2π. The intensity ratio of the ZVD shaper is given by I_1:I_2:I_3 = 1:2:1. Consequently, $I_1+I_2+I_3 = 0$ and $A_1+A_2+A_3 = 1$.

To enhance the robustness of the input shaper, the Zero Vibration Derivative (ZVD) scheme employs a se–quence of three impulses designed with the following parameters:

$$\begin{cases} A_1 = \dfrac{1}{1+2K+K^2}, t_1 = 0 \\ A_2 = \dfrac{2K}{1+2K+K^2}, t_2 = \dfrac{\pi}{\omega_d} \\ A_3 = \dfrac{K^2}{1+2K+K^2}, t_3 = \dfrac{2\pi}{\omega_d} \end{cases} \quad (14)$$

where: $K = e^{\frac{-\zeta\pi}{\sqrt{1-\zeta^2}}}$ and $\omega_d = \omega\sqrt{1-\zeta^2}$.

During the payload lifting/lowering process, the cable length l will be changed, which will cause time-varying vibration frequencies. This paper proposed using the average operating cable length-ZVD (AOL-ZVD) shaper, of which the vibration frequency is calculated using the average of all operated cable lengths.

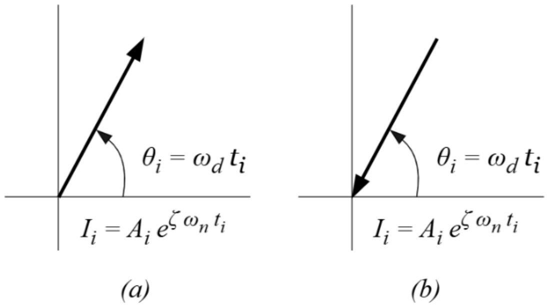

Figure 4. Response of impulse vectors

a) Positive impulse b) Negative impulse.

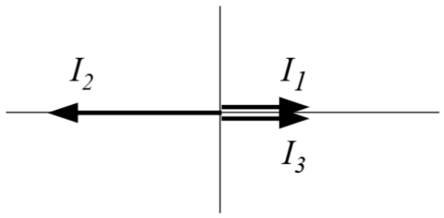

Figure 5. Impulse Vector Diagram of the ZVD Shaper.

3.3 Trajectory planning

The construction of the reference trajectory for both position and cable length aims to ensure smooth motor operation, minimize sudden impacts, and protect the components of the system. This allows the crane's start and stop processes to occur smoothly and in a controlled manner. In this paper, the reference trajectory for position and cable length is selected based on the following expressions:

$$\begin{cases} x_{ref} = x_d\left(1-e^{-8.33t^3}\right) \\ l_{ref} = \left(l_{\max} - l_{\min}\right)\left(1-e^{-8.33t^3}\right) + l_{\min} \end{cases} \quad (15)$$

where:

- x_{ref} is the reference value for horizontal trolley position control.
- l_{ref} is the reference value for cable length control.
- x_d is the desired trolley position along the horizontal axis.
- l_{max} is the maximum cable length (corresponding to the lowest load position).
- l_{min} is the minimum cable length (corresponding to the highest load position).

4. SIMULATION AND EXPERIMENT RESULTS

4.1 Simulation

In this simulation section, the parameters of the overhead crane are shown in Table 1. Here, the target trolley position in the horizontal direction is set to 1m, and the cable length varies within the range of 0.3m – 0.8m to meet the requirements of load lifting and lowering while ensuring minimal oscillation. The initial load position is at the lowest point with a rope length of $l_{\max}$ = 0.8m. When encountering an obstacle, the load is lifted to its highest position, reducing the rope length to $l_{\min}$ = 0.3m, then lowered back to l = 0.8m after clearance. These processes are controlled by two ADRC controllers operating simultaneously for both position and rope length.

From (15), the reference trajectory for the horizontal position and cable length is constructed and illustrated in Figure 6. Settling time is chosen as T_{settle} = 3 seconds for the ADRC position controller and T_{settle} = 1 second for the ADRC cable length controller. In both cases, the observer pole is set to $S^{ESO} = 100 \cdot s^{CL}$ to enhance disturbance rejection performance. For comparison, the input shaping - ZVD algorithm is simulated with three cable length values: the minimum $l_{\min}$ = 0.3m, the maximum $l_{\max}$ = 0.8m, and the average l_{avg} = 0.55m. Due to the lack of precise damping data and the fact that the actual experimental setup exhibits only small damping (primarily caused by mechanical friction), the damping ratio ζ was assumed to be zero during the computation of the input shapers. This simplification is commonly used in the design of input shapers when the system damping is small and does not significantly affect vibration suppression performance. The natural frequency of an individual pendulum will be evaluated utilizing the formula $\omega = \sqrt{g/l}$. The parameters of the ZVD shapers are listed in Table 2 respectively. The simulation results of the swing angle for these three cases of ZVD are presented in Figure 7.

The simulation results in Figure 7 show that applying the input shaping - ZVD algorithm with the average cable length achieves the optimal performance. Specifically, the maximum oscillation amplitude reaches only 3.74°, and the vibration reduction rate attains the highest level, up to 94.33%. Compared to the cases using the minimum cable length $l_{\min}$ and the maximum cable length $l_{\max}$, this method exhibits the best capability in eliminating residual vibrations, enabling the system to reach a stable state more quickly.

Table 1. Overhead Crane System Parameters

Parameter	Value
m_t	5 [Kg]
m_p	2.5 [Kg]
l	0.3-0.8 [m]
b_x	25 [Ns/m]
b_l	50 [Ns/m]
c_0	0.05 [Nms/rad]

Table 2. ZVD Shaper Parameters

Parameter	$l_{\max}$	$l_{\min}$	l_{avg}
A_1	0.25	0.25	0.25
A_2	0.5	0.5	0.5
A_3	0.25	0.25	0.25
t_1	0	0	0
t_2	0.8971	0.5494	0.7439
t_3	1.7943	1.0988	1.4877

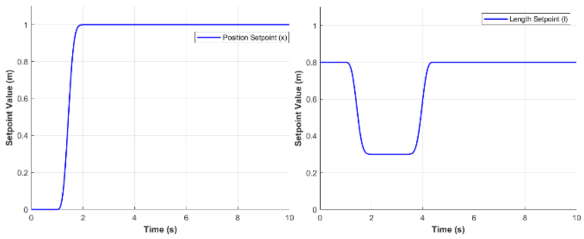

Figure 6. Trajectories of Trolley and Payload Positions.

From Figures 8 and 9, the results indicate that in the scenario involving driving the trolley to a 1m position, both ADRC and ADRC combined AOL-ZVD perform well with zero overshoot. However, the input shaping made the hybrid controller's response slower, as shown in Table 3. In contrast, the input in the case of ADRC AOL-ZVD is smoother than that of ADRC.

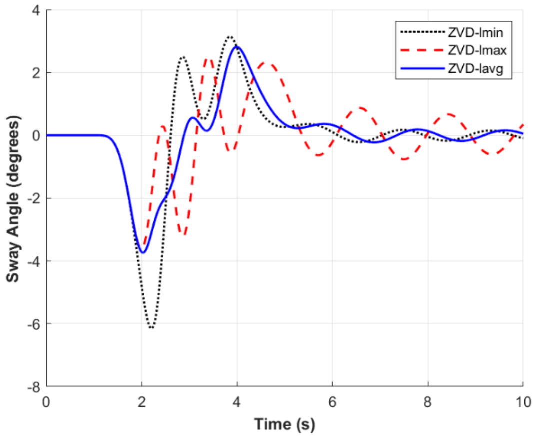

Figure 7. Sway Angle Response for Various Scenarios.

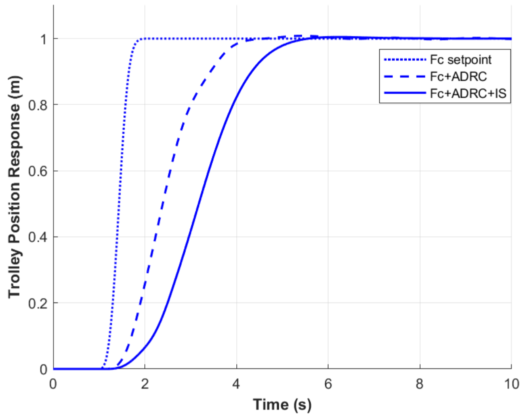

Figure 8. Simulation trolley position response.

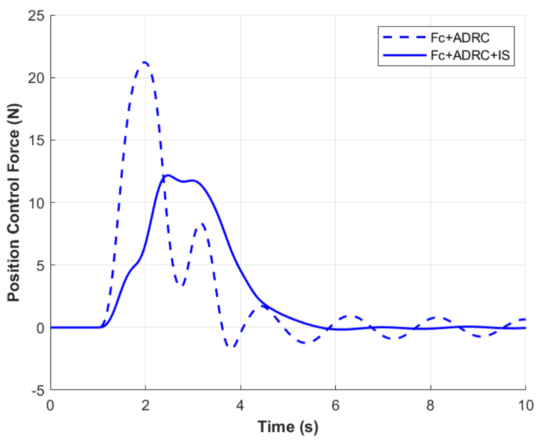

Figure 9. Simulation of position control force.

The cable length response can be observed in Figure 10 and Figure 11. With the AOL-ZVD, the payload sway angle vibration is significantly reduced. Mean–while, with the function-based reference trajectory, the proposed control minimizes residual oscillations and improves control performance.

Table 3. System Response Simulation Results

Settling time of trolley position (s)	ADRC	2.56
	ADRC+ZVD	3.58
Length Response (s)		01.09
Peak Position Control Force (N)	ADRC	21.22
	ADRC+ZVD	12.18
Peak Cable Force (N)		39.63
Peak Sway Angle (°)	ADRC	16.75
	ADRC+ZVD	3.74

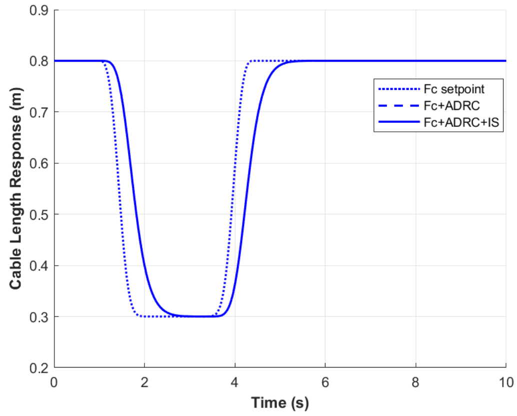

Figure 10. Simulation cable length response

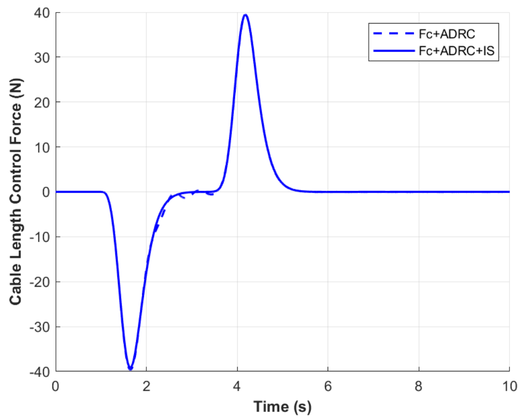

Figure 11. Simulation cable control force.

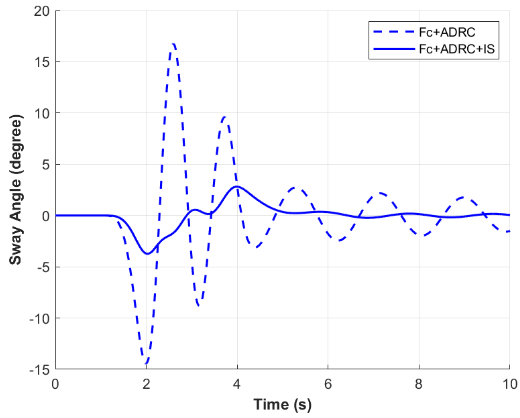

Figure 12. Simulation payload sway angle response.

4.2 Experiment validation

In this section, experiments are carried out using a 2D experimental overhead crane to validate the efficacy of the proposed approach, as illustrated in Figure 13. The system consists of a crane mechanism with an adjus–table rope length, designed to simulate real-world load transportation scenarios.

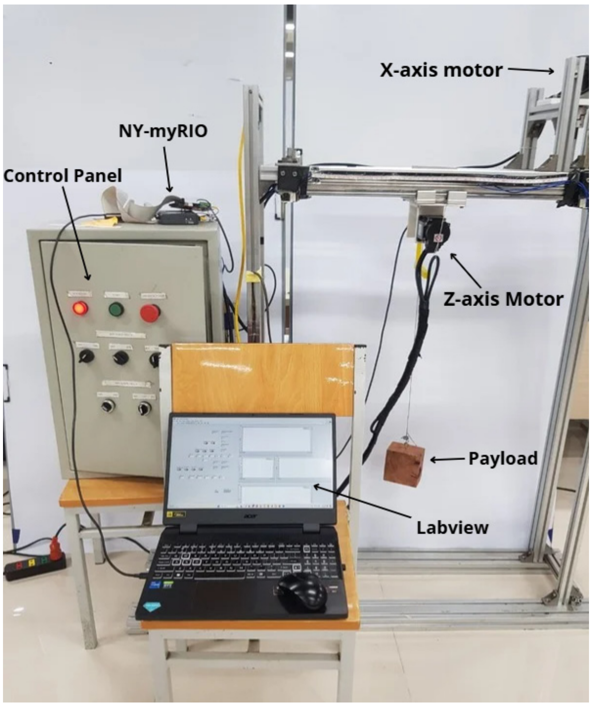

Figure 13. Experimental testbed for overhead crane control.

With the simulation results as above, using a trajec–tory setpoint in the form of a function to smooth the in–put will provide better performance. However, due to limitations in the physical structure of the test model and the travel distance along the x-axis, the experiment will be conducted using a unit pulse input signal, with a target distance of x = 40cm, while the rope length is raised from the lowest position of l = 50cm to the highest position of l = 20cm. The parameters of the ZVD input shaper, based on the average rope length method, are provided in Table 4. In addition, the settling time T_{settle} = 3.5 seconds for the ADRC controller controlling the position, T_{settle} = 1 second for the ADRC controller controlling the rope length, with the observer gain set to S^{ESO} = 100 and the control voltage is limited within the range [−10V,10V]. The experimental results are presented from Figure 14 to Figure 18.

Along with the calculated data, the time for the trolley to reach the target position x = 40cm is 3.1 seconds, while the time for the trolley to stabilize at the target position is 3.53 seconds. The shortest time for the cable length to reach the target value is 0.78 seconds, and the time for the cable length to stabilize at the target value is 0.975 seconds.

Furthermore, the control voltage remains within the allowable range of [−10V,10V] and does not exhibit sudden fluctuations that could destabilize the system. The damping ratio of the swing angle reaches 94.25%, which is consistent with the obtained simulation results.

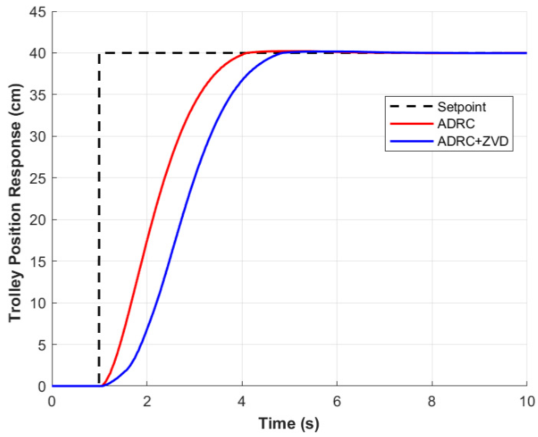

Figure 14. Experiment: trolley position response.

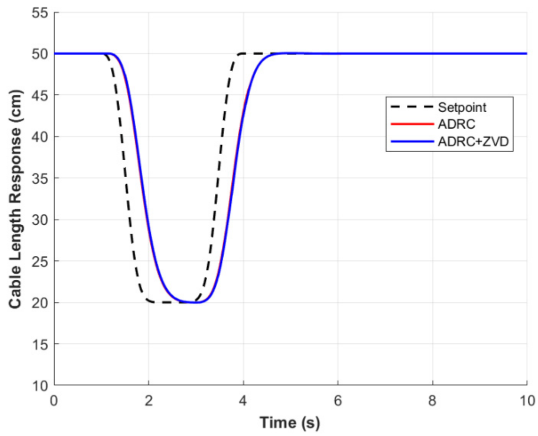

Figure 15. Experiment with cable length response.

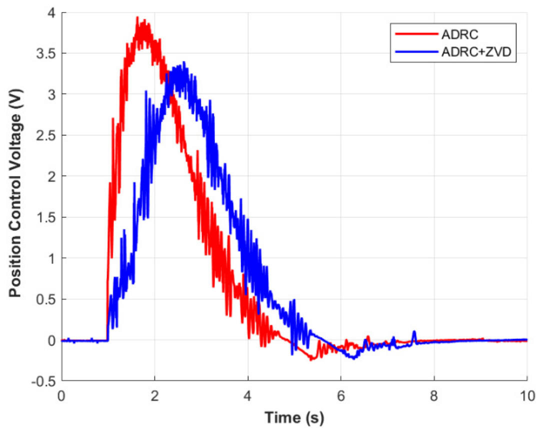

Figure 16. Position control voltage

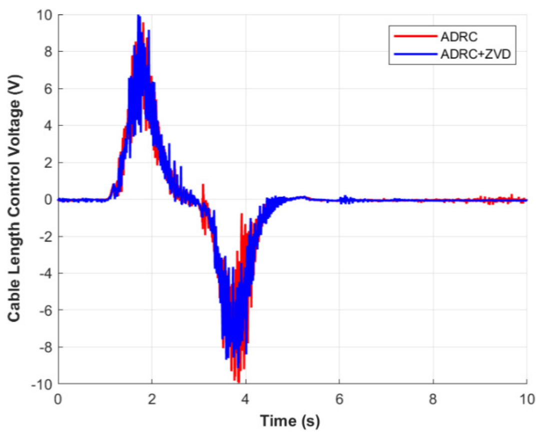

Figure 17. Experiment with cable length and control voltage.

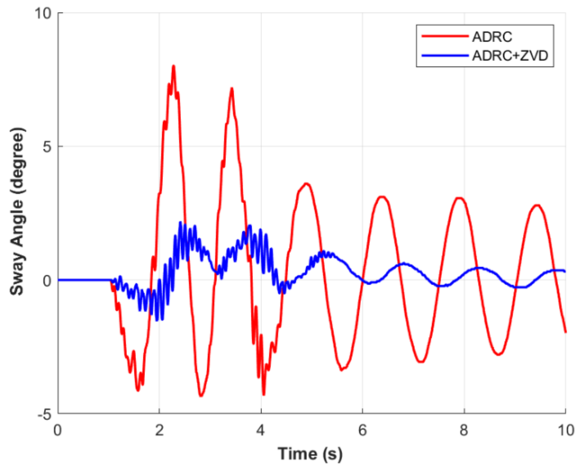

Figure 18. Experiment payload sway angle response.

Table 4. Experimental ZVD Shaper Parameters

Parameter	l_{avg}
A_1	0.25
A_2	0.5
A_3	0.25
t_1	0
t_2	0.5934
t_3	1.1868

5. CONCLUSIONS

This study successfully implemented a hybrid control strategy that combines Active Disturbance Rejection Control (ADRC) with Zero Vibration Derivative (ZVD) input shaping for an under actuated overhead crane system with variable cable length. The proposed app–roach achieves notable improvements in both position control performance and oscillation suppression. By employing a function-based reference trajectory, the input signal is smoothed effectively, resulting in good system response and reduced residual swing. Simul–taneously, the ZVD input shaper mitigates the impact of excitation impulses, leading to optimized control signals and enhanced system stability. Compared to conven–tional control strategies such as PID controllers that often rely heavily on accurate modeling and exhibit limited robustness, the proposed method demonstrates strong disturbance rejection capability and does not require precise knowledge of system parameters. Simu–lation and experimental results confirm that ADRC significantly enhances the robustness and accuracy of position and cable length control while maintaining system stability in the presence of sudden disturbances and parameter variations. These contributions represent a meaningful advancement over previous studies by offering a more adaptable and model-independent con–trol solution for crane systems. The integration of ADRC and input shaping proves especially valuable for industrial automation applications where precision, safety, and system adaptability are critical.

ACKNOWLEDGMENT

This research is funded by Hanoi University of Science and Technology (HUST) under project number T2024-PC-062.

REFERENCES

[1] Singhose, W. E., Lawrence, J., Sorensen, K. L. Dooroo, K. Applications and educational uses of crane oscillation control, FME Transactions, 34: 175–183, 2006.

[2] Mojallizadeh, M. R.,Brogliato, B. Prieur, C.: Mo–deling and control of overhead cranes: A tutorial overview and perspectives, Annual Reviews in Control, 56:100877, 2023.

[3] Wahrburg, A., Jurvanen, J., Niemela, M., Holmberg, M.: Input shaping for non-zero initial conditions and arbitrary input signals with an application to overhead crane control,in 2022 IEEE 17th International Conference on Advanced Motion Control (AMC), pages 36–41. IEEE, 2022.

[4] Abdullah Mohammed, A., Alghanim, K., Taheri Andani, M.: An adjustable zero vibration input shaping control scheme for overhead crane systems, Shock and Vibration, 2020(1):7879839.

[5] Zhang, Z., Wu, Y., Huang, J.: Differentialflatness-based finite-time anti-swing control of under–actuated crane systems, Nonlinear Dynamics, 87, 02 2017.

[6] Akira, A.: Non-linear control technique of a pendu–lum via cable length manipulation: Application of particle swarm optimization to controller design, FME Transactions, 41:265–270, 2013.

[7] Sun, N., Yang, T., Fang, Y., Wu, Y., Chen, H.: Transportation control of double-pendulum cranes with a nonlinear quasi-pid scheme: Design and experiments, IEEE Transactions on Systems, Man, and Cybernetics: Systems, 49(7):1408–1418, 2019.

[8] Chen, H., Fang, Y., Sun, N.: A swing constraint guaranteed mpc algorithm for underactuated over–head cranes. IEEE/ASME Transactions on Mechat–ronics, 21(5):2543–2555, 2016.

[9] Chang, C. Y.: Adaptive Fuzzy Controller of the Overhead Cranes with Nonlinear Disturbance, IEEE Transactions on Industrial Informatics, vol. 3, no. 2, pp. 164-172, May 2007.

[10] Zrnic, N., Petkovic, Z. and Bosnjak, S. Automation of ship-to-shore container cranes: A review of state-of-the-art, FME Transactions, 33:111–121, 2005.

[11] Solazzi, L., Zrnic, N.: Dynamic analyses of gantry crane under several trolley and payload movements, FME Transactions, 48:281–286, 2020.

[12] Gao, Z., Huang, Y., Han, J.: An alternative para–digm for control system design, in Proceedings of the 40th IEEE Conference on Decision and Control (Cat. No.01CH37228), volume 5, pp. 4578– 4585, 2001.

[13] Han, J.: From pid to active disturbance rejection control, IEEE Transactions on Industrial Elect–ronics, 56(3):900–906, 2009.

[14] Gao, Z.: Scaling and bandwidth-parameterization based controller tuning,in Proceedings of the 2003 American Control Conference, pages 4989–4996, 2003.

[15] Chen, H., Yang, P., Geng, Y.: A time optimal trajectory planning method for overhead cranes with obstacle avoidance,in 2019 IEEE/ASME International Conference on Advanced Intelligent Mechatronics (AIM), pages 697–701, 2019.

[16] Herbst, G.: A Simulative Study on Active Disturbance Rejection Control (ADRC) as a Control Tool for Practitioners, Electronics, 2(3):246–279, 2013.

[17] Singer, N. C., Seering, W. P.:Preshaping command inputs to reduce system vibration, Journal of Dynamic Systems, Measurement, and Control, 112(1): 76–82, 03 1990.

[18] Sorensen, K. L.,Hekman,K. andSinghose, W. E.: Finitestate input shaping, IEEE Transactions on Control Systems Technology, 18(3):664–672, 2010.

[19] Kang, C. -G.: Impulse vectors for input-shaping control: A mathematical tool to design and analyzeinput shapers, IEEE Control Systems Magazine, 39(4):40–55, 2019.

NOMENCLATURE

x	trolley position
l	cable length
θ	sway angle of the payload
m_t	trolley mass
m_p	payload mass
b_x	damping coefficient along the x-axis
b_l	damping coefficient along the y-axis
c_0	rotational damping coefficient
T_{settle}	2% settling time

Greek symbols

ζ	damping ratio
ω_n	natural frequency

Acronyms and Abbreviations

ADRC	Active Disturbance Rejection Control
ESO	Extended State Observer
PID	Proportional–Integral–Derivative
ZVD	Zero Vibration Derivative
AOL	Average Operating Length

ПОБОЉШАНО УПРАВЉАЊЕ НАДЗЕМНОМ ДИЗАЛИЦОМ КОРИШЋЕЊЕМ ADRC И ZVD ОБЛИКОВАЊА УЛАЗА СА ПЛАНИРАЊЕМ ПУТАЊЕ

В.Д. Нгујен, М.Д. Дуонг, Т.Х. До

Управљање надземном дизалицом са временски променљивом дужином кабла представља значајне изазове, посебно у одржавању тачног позиционирања колица уз минимизирање преосталих осцилација корисног терета изазваних операцијама подизања и спуштања. Овај рад предлаже хибридни приступ управљању који комбинује активно управљање одбацивањем поремећаја (ADRC) са обликовањем улаза са нултим вибрацијама (ZVD) како би се решили ови проблеми. ADRC побољшава робусност система на спољашње поремећаје и несигурности модела, пружајући стабилне перформансе праћења. Међутим, због својих ограничења у потпуном сузбијању преосталих осцилација, ZVD обликовач улаза је интегрисан како би се смањило њихање корисног терета. Да би се додатно оптимизовале перформансе обликовања при променљивим дужинама ужета, користи се стратегија просечне дужине кабла за подешавање параметара. Поред тога, развијена је шема планирања референтне путање за углађивање улазних команди, смањење изненадних удараца, индукованих осцилација и побољшање укупне стабилности система током рада дизалице.